Comparative Medicine
Copyright 2009
by the American Association for Laboratory Animal Science

Vol 59, No 1
February 2009
Pages 37–45

# Use of Low-Molecular–Weight Heparin to Decrease Mortality in Mice after Intracardiac Injection of Tumor Cells

**Kim L Stocking,[1,*] Jon C Jones,[2] Nancy E Everds,[3] Bernard S Buetow,[3,†] Martine P Roudier,[3] and Robert E Miller[2]**

**Intracardiac injection of human tumor cells into anesthetized nude mice is an established model of bone metastasis. However, intracardiac injection of some human tumor cell lines cause acute neurologic signs and high mortality, making some potentially relevant tumor cell lines unusable for investigation. We showed that intracardiac injection of tumor cells can induce a hypercoagulable state leading to platelet consumption and thromboemboli formation and that pretreatment with intravenous injection of low-molecular–weight heparin (LMWH; enoxaparin) blocks this state. In addition, intravenous injection of enoxaparin before intracardiac injection with 2 different small-cell lung carcinoma lines, H1975 and H2126, dramatically decreased mouse mortality while still generating bone metastases. Therefore, reduction of mortality by pretreatment with LMWH increases the types of cells that can be studied in this metastasis model and decreases the number of animals used.**

**Abbreviations:** APTT, activated partial thromboplastin time; BLI, bioluminescent imaging; CBC, complete blood count; DIC, disseminated intravascular coagulation; H1975luc, H1975 cell line tagged with lucerifase–green fluorescent protein; H2126luc, H2126 cell line tagged with lucerifase–green fluorescent protein; LMWH, low-molecular–weight heparin; PT, prothrombin time; UFH, unfractionated heparin.

Research using animal models mimicking the metastasis of human tumors to bone is critical for the development of cancer therapeutics. Bone metastases are present in almost all people who die of cancer and are more likely to occur with breast, prostate, lung, kidney, and thyroid cancers.[1,24] In patients with advanced breast and prostate cancers, much of the tumor burden at the time of death will be found in bone.[20] The pattern of bone metastases can range from purely destructive (osteolytic) to mostly osteoblastic (bone-forming) lesions. Osteolysis is accompanied by pain, bone fragility, and increased susceptibility to pathologic fracture. In osteolytic metastasis, a 2-way interaction between tumor cells and osteoclasts in the bone microenvironment leading to continued osteolysis and tumor growth is suspected.[20] Current therapies for bone metastases, such as bisphosphonates, are directed at inhibiting bone resorption, but other therapies are in development that specifically target tumor cell or osteoclast factors involved in the 2-way cycle between tumor growth and osteolysis.[18]

Bone metastasis is rare in mouse models of spontaneous mammary and prostate carcinomas, experimentally implanted animal tumor models (such as syngeneic and xenograft tumors), and chemical or transgenic induction of mammary and prostate carcinomas. To increase the frequency of bone metastases, injection techniques using either orthotopic tumor cell injection into mammary glands or prostate or intracardiac injection of human tumor cell lines into the left ventricle of nude mice have been developed.[5,14,25,31] In contrast to the late stage, low incidence of metastasis after orthotopic injection, intracardiac injection of human tumor cell lines results in much higher rates of bone metastasis at an early stage in the disease, with osteolytic metastases to the metaphyses of long bones.[6,23] Development of osteolytic lesions in this model can be monitored by various methods, including radiography and, more recently, in vivo bioluminescent imaging (BLI) using lucerifase-tagged tumor cells. Bioluminescent imaging detects micrometastatic lesions and allows for serial in vivo monitoring of bone metastases.[9-11] After a BLI study, bone metastases can be assessed histologically, with tumor foci typically seen in the femur or tibia.

Bone metastasis models using the intracardiac tumor injection technique have been primarily focused on a few breast (for example, MDA-MB-231) and prostate models (for example, PC3), but additional models of other tumors that interact with bone (especially lung carcinomas) need to be developed.[24,30] Intracardiac injection of some nonsmall cell lung carcinoma tumor cell lines have led to stroke-like clinical signs, including head tilt, spinning, and failure to recover from anesthesia after intracardiac injection.[15] We postulated that the stroke-like clinical signs and mortality were due to thromboembolism formation immediately after intracardiac tumor cell injection.

Tumor cells have procoagulant activity. Procoagulants, such as tissue factor, may be increased on the surface of or secreted into the blood by cancer cells, leading to changes in the clotting cascade.[13] Approximately 15% of all cancer patients are affected by thromboembolic disease, including superficial and deep-vein thrombosis, arterial thrombosis and embolism, pulmonary emboli, and thrombosis of venous access devices.[12,13] Anticoagulant

*Received: 22 May 2008. Revision requested: 02 Jul 2008. Accepted: 10 Aug 2008.*
*[1]Comparative Animal Research and Departments of [2]Oncology, and [3]Pathology, Amgen Corporation, Seattle, Washington.*
*[†]Current affiliation: Anatomic Pathology, Wyeth Research, Chazy, New York.*
**Corresponding author. Email:kstock01@amgen.com*

treatments used clinically to prevent thrombi and thromboemboli include warfarin, unfractionated heparin (UFH), and low-molecular–weight heparins (LMWH), such as enoxaparin (Lovenox, Sanofi Aventis, Bridgewater, NJ) and dalteparin (Fragmin, Pfizer, New York, NY). LMWHs are prepared through chemical, hydrolytic, or enzymatic degradation of unfractionated heparin.[13] Both UFH and LMWH exert their anticoagulant effects by binding to antithrombin and causing a confrontational change. This change increases the interaction of antithrombin with thrombin (IIa) and activated factors X (Xa) and IX (IXa), leading to inhibition of clotting.[8,28]

LMWHs decrease the formation of thromboembolism and subsequent mortality in several murine models of thromboembolism and disseminated intravascular coagulation (DIC). In the murine model of thrombin-induced thromboembolism, massive deposition of intravascular fibrin—mainly within the pulmonary arteries—causes death within 5 minutes after thrombin injection.[16,22] Both UFH and LMWH inhibit thrombin and prevent mortality in this model, but bleeding times and activated partial prothrombin time (APPT) are less prolonged with LMWH.[16] LMWH is also effective in preventing murine DIC in a lipopolysaccharide model, in which mice given 2 injections of lipopolysaccharide develop DIC, multiple organ failure, and die. Mice given LMWH before lipopolysaccharide administration have fewer lung and liver microthrombi and greater survival than do mice not given LMWH.[26,27]

Here, we evaluated the use of LMWH in mice to prevent morbidity and mortality associated with intracardiac injection of human tumor cell lines. We determined that thromboembolism occurred in intracardiac tumor-challenged mice and that LMWH blocked thromboembolism. We also determined the effect of LMWH on animal survival and subsequent development of bone metastasis in this mouse model.

## Materials and Methods

**Reagents.** Nonsmall cell lung cancer cell lines H1975 and H2126 (American Type Culture Collection, Manassas, VA) were transformed to express luciferase and green fluorescent protein by using a lentiviral vector with a murine EF1a promoter, pLV411G. Transduced cells were sorted for expression of green fluorescent protein and placed into culture in RPMI media (Invitrogen, Grand Island, NY) with 10% fetal calf serum at 5% $CO_2$, 37 °C. These lucerifase-tagged cell lines are referred to as H1975luc and H2126luc. Cell lines were tested negative for *Mycoplasma* species and rodent viral pathogens (Sendai, mouse hepatitis virus, pneumonia virus of mice, minute virus of mice, mouse parvovirus, reovirus 3, mouse rotavirus, murine norovirus, *Ectromelia* virus, lymphocytic choriomeningitis virus, polyoma virus, K virus, mouse adenovirus, mouse cytomegalovirus, lactate dehydrogenase-elevating virus, mouse thymic virus, Hantaan virus, Kilham rat virus, Toolan H1 virus, rat parvovirus, rat cytomegalovirus, rat coronavirus, rat minute virus, sialodacryoadenitis virus, Seoul virus, Theiler murine encephalomyelitis virus, Theiler murine encephalomyelitis like virus) by PCR assays and passaged aseptically in a biological safety cabinet. For intracardiac injection, the cells were harvested from T175 culture flasks (Corning, Corning, NY) after a 5-min treatment with trypsin–EDTA (Invitrogen), counted by using an automated cell counter (Vi-Cell, Becton Dickinson, Franklin Lakes, NJ), and adjusted to appropriate numbers of cells per milliliter in serum-free RPMI media.

Enoxaparin sodium (Lovenox, Sanofi Aventis) was diluted in 0.9% sterile saline to a concentration of 1 mg/mL and administered at 10 mg/kg intravenously into the tail vein. The enoxaparin dose was chosen based on a previously published study using enoxaparin intravenously in mice in a B16 melanoma mouse model of metastasis.[19]

Firefly D-luciferin (Xenogen, Alameda, CA) was diluted to 15 mg/mL and stored at –80 °C and protected from light until thawed and administered at 150 mg/kg intraperitoneally.

**Animals.** Female CrTac:NCr-*Foxn1*$^{nu}$ were obtained from Taconic (Germantown, NY, and Cambridge City, IN). Mice were 4 to 8 wk old at the start of the experiments. All experimental procedures were approved by the institutional animal care and use committee at an AAALAC-accredited facility and adhered to *the Guide for the Care and Use of Laboratory Animals*.[21]

Mice were housed 5 per cage in sterile individually ventilated microisolation caging with corncob bedding and provided irradiated feed (5053, Purina, St Louis, MO) and reverse-osmosis–purified water ad libitum. Temperature was maintained at 20 to 22 °C, with humidity at 30% to 60% and a 12:12-h light:dark cycle. Mice were housed in a specific pathogen-free facility where quarterly sentinel surveillance was done. Sentinel mice were negative for respiratory and enteric bacterial pathogens, *Helicobacter* spp., *Mycoplasma pulmonis*, Sendai virus, murine norovirus, mouse hepatitis virus, pneumonia virus of mice, minute virus of mice, mouse parvovirus types 1 through 4, reovirus 1 and 3, mouse rotavirus, *Ectromelia* virus, lymphocytic choriomeningitis virus, polyoma virus, K virus, mouse adenovirus types 1 and 2, mouse cytomegalovirus, lactate dehydrogenase-elevating virus, mouse thymic virus, Hantaan virus, Seoul virus, Theiler murine encephalomyelitis virus, endoparasites, and ectoparasites.

**Intracardiac injections.** Mice were anesthetized with 90 mg/kg ketamine and 10 mg/kg xylazine intraperitoneally prior to the intracardiac injections. Mice were placed in dorsal recumbency and injected in the left ventricle with $1 \times 10^6$ lucerifase-tagged tumor cells in 100 µL serum-free media by using a 0.5-mL tuberculin syringe with a 27-gauge needle (Beckton Dickinson). Sterile skin prep was not done prior to injection, but the injection needle was changed between animals. The dose for tumor cells was based on preliminary experiments that showed survival but inconsistent tumor metastases after intracardiac injection of $1 \times 10^5$ H1975luc cells (data not shown). To assess the accuracy of intracardiac injection, mice were imaged (IVIS 200, Xenogen) 4 minutes after intraperitoneal injection with 150 mg/kg D-luciferin. D -Luciferin interacts with the lucerifase-tagged tumor cells, and accurate intracardiac injection results in distribution of bioluminescence throughout the animal. Mice were monitored until recovery from anesthesia, and any mice exhibiting neurologic clinical signs were euthanized. Failure to regain consciousness after anesthesia or to survive beyond the first few days after tumor challenge was noted.

**Imaging.** Development and extent of metastasis was monitored by in vivo BLI to detect bioluminescence of human tumor cell lines expressing firefly lucerifase and green fluorescent protein. Mice were injected with D-luciferin (150 mg/kg IP) and anesthetized by exposure to 3% isoflurane in $O_2$. Mice were imaged under isoflurane anesthesia, with dorsal and ventral images collected at 9 and 11 min after luciferin injection, respectively. Images were collected twice weekly after the first week until study termination. Images were gated for regions of interest that included

the whole body, both hindlimbs, and the head area, and images were analyzed by using Living Image software (Xenogen).[11] Areas were considered to be positive for tumor if the luminescent signal exceeded a manually adjusted low minimal threshold. In vivo bioluminescence was quantified, and the mean number of photons per second was calculated at each time point.

Development and progression of osteolytic bone lesions were monitored by radiography. Immediately after bioluminescent imaging, mice were placed singly in dorsal recumbency into the radiography system (MX20, Faxitron X-ray Corporation, Wheeling, IL). Digital radiographic images of hindlimbs and pelvic areas were captured by using a duration of 10 s, magnification of ×4, and beam energy of 26 kV.

**Investigation of thromboembolism.** Twenty mice received 10 mg/kg enoxaparin intravenously 10 min prior to intracardiac injection of $1 \times 10^6$ H2126luc cells, and another 20 mice received no treatment prior to intracardiac tumor cell injection of $1 \times 10^6$ H2126luc cells. Mice were injected intraperitoneally with 150 mg/kg D-luciferin, and successful intracardiac injection was verified by BLI. Immediately after imaging, blood was collected by cardiocentesis and placed into $K_2$EDTA blood tubes (Becton Dickinson) for complete blood count (CBC) or into sodium citrate (1.5-mL microfuge tubes; 1:10 v/v) for determination of coagulation parameters. Blood was collected from 10 mice from each group (untreated and enoxaparin-pretreated) for CBC and from the remaining 10 mice for coagulation assays. In addition, 10 mice from each group were evaluated histologically for thromboembolism. All mice were under ketamine–xylazine anesthesia at the time of cardiocentesis and were euthanized immediately afterward by cervical dislocation.

All blood samples were evaluated for clotting by visual examination. Plasma samples for coagulation measurements were frozen at –80 ºC until analyzed. Complete blood counts, including reticulocytes, were determined on an automated hematology analyzer (Advia 120, Siemens, Tarrytown, NY) or from microscopic evaluation of the blood smear. Wright–Giemsa-stained blood smears from all animals were examined microscopically for confirmation of automated results. Coagulation times [prothrombin time (PT) and APTT] and fibrinogen concentrations were determined on an automated coagulation analyzer (ACL Elite Pro, Beckman Coulter, Miami, FL).

To assess thromboembolism formation, selected tissues (brain, liver, kidney, lung, heart and tibia) were collected at necropsy and placed in 10% formalin solution. Tissues were paraffin embedded, sectioned and stained with hematoxylin and eosin. Slides were evaluated microscopically for formation of thromboemboli. To better visualize and characterize thrombi that were present, a subset of slides was stained with phosphotungstic acid hematoxylin.

**Effect of LMWH on survival and metastases.** Ten mice were given $1 \times 10^6$ H1975luc cells by intracardiac injection. An additional 10 mice were given 10 mg/kg enoxaparin intravenously in the tail vein 10 min prior to administration of $1 \times 10^6$ H1975luc cells by intracardiac injection. In a separate study using H2126luc cells, a group of 15 mice was given 10 mg/kg enoxaparin intravenously in the tail vein 10 min prior to intracardiac injection of $1 \times 10^6$ H2126luc cells. A nonenoxaparin pretreated group was not included in the H2126luc study because of the 100% mortality seen in the thromboembolism study (see previous section). Successful intracardiac injection was assessed by BLI, and only mice with evidence of accurate injection were included in the study. Mortality and neurologic clinical signs were monitored, and surviving mice were followed as long as 29 d for development of metastases and osteolytic lesions in the hindlimbs. Body weight determinations and imaging typically occurred twice weekly, with imaging days determined by personnel schedules and by how quickly metastatic lesions developed. Mice were scheduled for euthanasia if they had weight loss exceeding 20% of prestudy body weight, showed evidence of paraplegia, or had severe osteolysis that resulted in bone fracture. Mice given H1975luc cells were anesthetized with isoflurane, weighed, and imaged by BLI on days 3, 6, 12, 15, 19, 22, 26, and 29 after intracardiac tumor challenge. In addition, the pelvic area and hindlimbs of each H1975luc -injected mouse were radiographed on days 22, 26, and 29 to monitor the development of osteolytic lesions. Mice given H2126luc cells were anesthetized with isoflurane, weighed, and imaged on days 8, 12, 15, 19, and 22 after tumor challenge. In addition, the pelvic area and hindlimbs of each H2126luc-injected mouse were radiographed on days 12, 19, and 22 to monitor the development of osteolytic lesions. Mice were euthanized by $CO_2$ followed by cervical dislocation. For histologic assessment of bone metastasis, both femurs and tibias were collected from each mouse, sectioned, and stained with hematoxylin and eosin and tartrate-resistant acidic phosphatase.

**Statistical analysis.** Growth curves from BLI data were evaluated by repeated-measures analysis of covariance of the log-transformed bioluminescence data by using Dunnett adjusted multiple comparisons. All statistical calculations were made through the use of JMP software version 7.0 interfaced with SAS version 9.1 (SAS Institute, Cary, NC). Single-point measurements were analyzed by 1-way ANOVA by using a Dunnett post test (JMP7, SAS Institute).

## Results

**Thromboembolism study.** All 20 enoxaparin-pretreated mice survived the 15 min needed to verify successful intracardiac injection of H2126luc tumor cells and to collect blood samples for either CBC or coagulation parameters. Without enoxaparin pretreatment, all 20 mice died within 5 to 10 min after intracardiac injection. Blood collection was attempted in moribund mice, but many of the blood samples clotted during collection. Due to clotted specimens in the untreated group, CBC were performed on only 5 of 10 hematology samples, and none of the coagulation samples were analyzed. No clotting was noted in any of the EDTA or citrated blood samples from enoxaparin-pretreated animals. Results of CBC from animals pretreated with enoxaparin were similar to expected values for mice.[7,17] Animals in the untreated group had significantly ($P = 0.002$) lower total white blood cell counts, with significantly fewer numbers of neutrophils ($P < 0.0001$), lymphocytes ($P = 0.02$), and eosinophils ($P = 0.0003$) when compared with values for the enoxaparin-pretreated group (Figure 1). Platelets counts were markedly and significantly ($P < 0.0001$) lower in the untreated group (Figure 2 A), with a significantly ($P = 0.0001$) but minimally higher mean platelet volume (Figure 2 B) and a significantly ($P < 0.0001$) but minimally lower mean platelet concentration (Figure 2 C). Neither platelet clumps nor large platelets were present on blood smears. Although coagulation tests were not available for mice not pretreated with enoxaparin, values for PT (mean, 6.8 ± 0.16 s) and fibrinogen (mean, 163 ± 27 mg/dL) from the enoxaparin-pretreated mice were similar to published reference intervals for mice (PT, 7.3 ± 0.4 s; fibrinogen, 230 ± 30

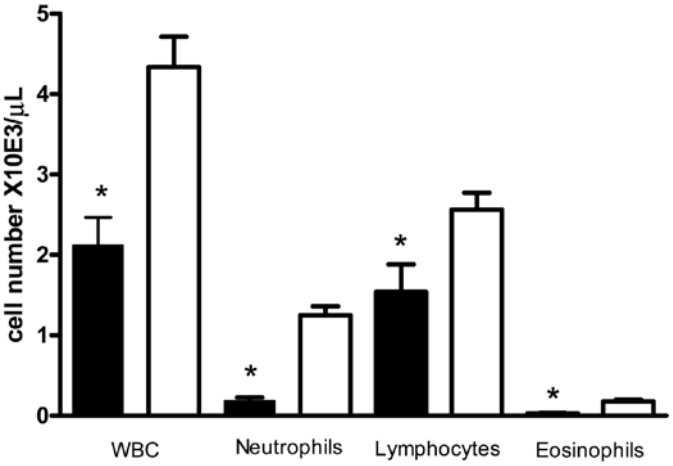


**Figure 1.** White blood cell counts (mean ± SEM) without (dark bars; n = 5) or with (white bars; n = 10) enoxaparin pretreatment. Untreated mice had significant (*, $P \leq 0.02$) decreases in total white blood cell (WBC), neutrophil, lymphocyte,and eosinophil counts.

mg/dL).[29] All APTT times for enoxaparin-pretreated mice were prolonged beyond the time limit of the coagulation analyzer (110 s; normal murine APTT, 22 ± 0.7 s).[29] Hematocrit and hemoglobin values were minimally but not significantly higher in the untreated group versus the enoxaparin-pretreated group ($P = 0.10$ and $P = 0.06$, respectively; Table 1).

Mice not pretreated with enoxaparin had clear histologic evidence of increased blood coagulability. The lungs of all 10 of these mice had numerous thromboemboli within many medium to small pulmonary vessels including alveolar capillaries (Figure 3 A, B). The thromboemboli were composed of platelets, fibrin, and generally low numbers of erythrocytes. Rarely, neoplastic cells were present within the thromboemboli. Rare (1 to 2 per tissue) small thrombi were present with the vasculature of the brain (4 of 10 mice) and kidney (3 of 10 mice). None of the 10 mice pretreated with enoxaparin had pulmonary (Figure 3 C, D) or brain thromboemboli, and only 2 mice had rare small renal thromboemboli. Other examined organs (liver, heart, tibia) did not have evidence of antemortem thrombus formation in either enoxaparin-pretreated or untreated mice.

**Effect of LMWH on survival and metastases.** Of 10 mice that did not receive enoxaparin prior to intracardiac injection with $1 \times 10^6$ H1975luc cells, 5 suffered stroke-like events and died immediately. The 5 remaining mice survived successful intracardiac injection and were included in the study. All mice receiving enoxaparin prior to challenge with $1 \times 10^6$ H1975luc cells survived intracardiac injection; however, 2 of those intracardiac injections were deemed unsuccessful by BLI, and those mice were not included in the study. Of the mice that received intracardiac injection of H2126luc tumor cells with enoxaparin pretreatment, 12 of the intracardiac injections were considered successful, and 10 of those 12 mice survived and continued on the study. The surviving H1975luc and H2126luc mice were monitored by BLI and radiography for development of metastases and osteolytic lesions in the hindlimbs. At day 19, 1 mouse in the H2126luc group had a pathologic fracture of the femur and therefore was euthanized. At day 22, body weights on the remaining 9 H2126luc mice had declined, and a progressive increase in bioluminescence and osteolytic lesions was noted, so the H2126luc study was terminated.

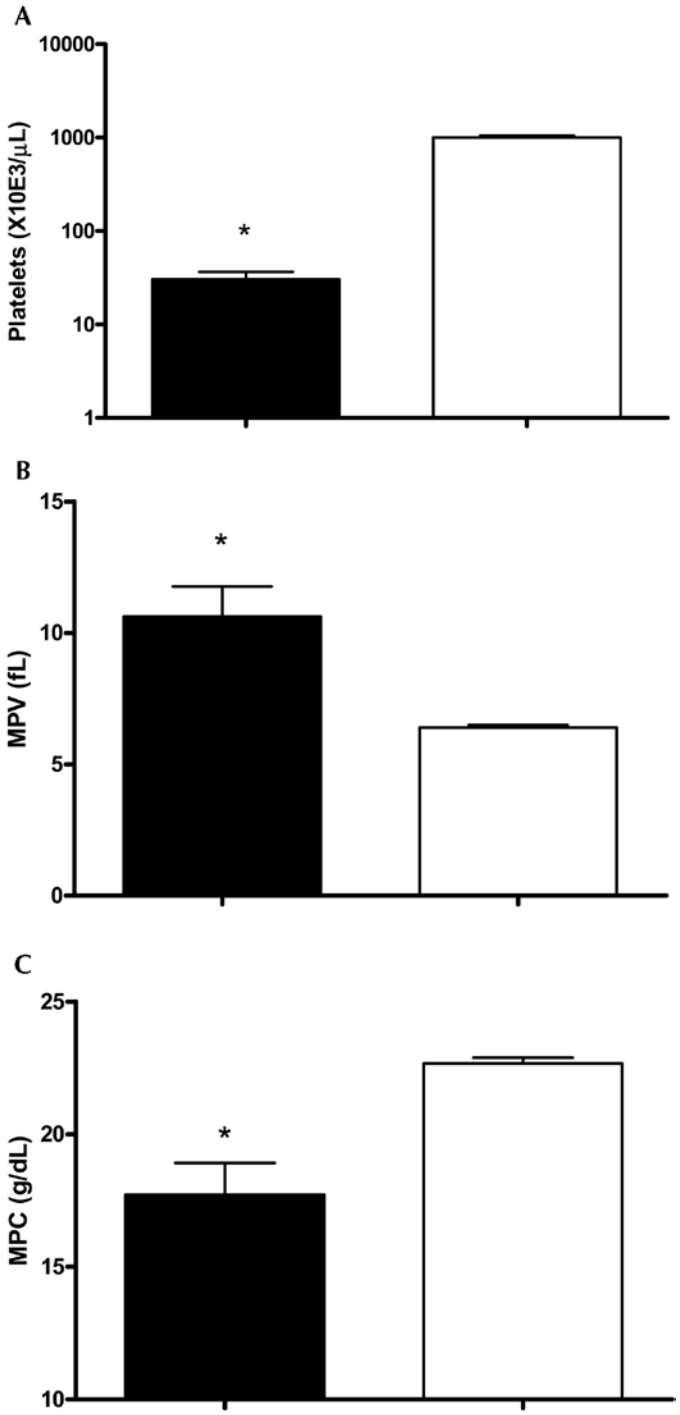


**Figure 2.** Platelet parameters (mean ± SEM) without (dark bars; n = 5) or with (white bars; n = 10) enoxaparin pretreatment. Untreated mice had significant (*, $P \leq 0.0001$) decreases in (A) platelet numbers and (C) mean platelet concentration (MPC), with a significant increase in (B) mean platelet volume (MPV).

Surviving H1975luc mice did not have any pathologic fractures, and body weight losses were acceptable until the end of the study on day 29.

Enoxaparin pretreatment of H1975luc mice had no effect on overall body weight loss as well as no effect on tumor burden

**Table 1.** Blood parameters in mice with and without enoxaparin pretreatment

| | Untreated | Enoxaparin-pretreated |
|---|---|---|
| Red blood cells (x10$^6$/μL) | 8.28 ± 0.22 | 7.85 ± 0.16 |
| Hemoglobin (g/dL) | 13.2 ± 0.4 | 12.3 ± 0.2 |
| Hematocrit (%) | 43.6 ± 1.2 | 41.3 ± 0.7 |
| White blood cells (x10$^3$/μL) | 2.12 ± 0.48[a] | 4.34 ± 0.34 |
| Neutrophils (x10$^3$/μL) | 0.18 ± 0.13[a] | 1.25 ± 0.09 |
| Lymphocytes (x10$^3$/μL) | 1.54 ± 0.31[a] | 2.56 ± 0.22 |
| Eosinophils (x10$^3$/μL) | 0.03 ± 0.02[a] | 0.18 ± 0.02 |
| Platelets (x10$^3$/μL) | 30 ± 61[b] | 1001 ± 43 |
| Mean platelet volume (fL) | 10.6 ± 0.6[b] | 6.4 ± 0.5 |
| Mean platelet concentration (g/dL) | 17.7 ± 1.2[b] | 22.7 ± 0.2 |

Data are given as mean ± SEM (no pretreatment, n = 5; enoxaparin pretreatment, n = 10)
[a]Values differ significantly at $P \leq 0.02$.
[b]Values differ significantly at $P \leq 0.0001$.

(whole body, hindlimb, and head) as measured by bioluminescence, radiography, and histology when compared with untreated H1975luc mice (Figure 4 A, B). The H2126luc mice showed a typical body weight loss pattern seen for this model, where body weight is maintained until osteolytic lesions become pronounced. A decrease in body weight along with the development of osteolytic lesions signaled the end of the study. Bioluminescent imaging showed substantial tumor burden by day 22 (Figure 5 A), and radiography and histology showed substantial osteolytic lesions in the hind limbs. Staining with tartrate-resistant acidic phosphatase showed osteoclasts at the bone–tumor interface (Figure 5 B). Histopathologic scoring of bone metastases in the H2126luc mice showed 1 to 5 tumor foci in each femur and tibia.

## Discussion

Because bone metastasis is common in human cancers, mouse models of bone metastasis are important in the development of effective treatments. Intracardiac injection of human tumor cell lines into nude mice results in multiple bone metastases and allows examination of the effects of potential therapeutics on tumors growing in the bone microenvironment. However, intracardiac injections of some human tumor cell lines cause neurologic clinical signs and high mortality in mice. Our previous work with the nonsmall cell lung carcinoma lines H1975luc and H2126luc resulted in 50% to 80% and 70% mortality, respectively (data not shown). In the few mice that survived, bioluminescence was present in bone, indicating that these cell lines could be useful in investigating metastases if mortality could be decreased. Continuing to conduct experiments with the high mortality rates would have required excessive numbers of animals, so we undertook a series of experiments to refine this bone metastasis model.

Approximately 15% of human patients with cancer suffer from thromboembolic disease. Treatment with UFH, LMWH, and warfarin has been used in cancer patients to prevent thrombosis. We hypothesized that the neurologic clinical signs and death after intracardiac tumor challenge in mice might be due to a hypercoagulable state that could be prevented by pretreatment with a LMWH.

In the thromboembolism study, CBC and coagulation parameters as well as histopathology were evaluated in untreated and enoxaparin-pretreated mice that received intracardiac injections of H2126luc tumor cells. Mice that were treated with enoxaparin before intracardiac tumor challenge had successful collection of blood for hematology and coagulation. All CBC and coagulation test results (except APTT) were similar to those expected in naïve mice, and no thromboemboli were noted in the lungs. Due to pharmacologic inhibition of the intrinsic clotting cascade by enoxaparin, times for APTT were prolonged beyond the time limit of the assay (110 s). The PT and fibrinogen concentration were slightly lower than the published means of normal mice. Differences between PT and fibrinogen results on this study and published reference intervals likely reflect methodologic biases.

In contrast, all mice that did not receive enoxaparin before intracardiac challenge with H2126luc cells had hypercoagulable blood, as indicated by clots in many of the collection syringes and blood collection tubes. The markedly lower platelets counts in untreated mice likely were due to consumption. Platelet consumption was indicated also by the large number of thromboemboli (primarily in the lungs) of untreated mice. The higher mean platelet volume seen in the untreated mice may have been due to release of large platelets or to platelet clumping, but neither platelet clumps nor large platelets were observed on blood smears. The lower mean platelet concentration seen in the untreated mice indicates a decrease in platelet granularity, probably due to activation. The untreated group also had a significant decrease in leukocytes due to decreases in lymphocytes, eosinophils, and neutrophils. The moderate decrease in neutrophils could be due to egress from the vasculature or to sequestration in capillary beds (or both).

In animal models of lipopolysaccharide-induced DIC, profound neutropenia occurs within 4 h, with most of the neutrophils preferentially sequestering to the lungs.[2-4,26,27] In our study, neutrophil sequestration was not noted in lung, liver, brain, heart, or kidney sections. Minimal increases in hematocrit and hemoglobin in the untreated group compared with the enoxaparin-pretreated group may be due to a dilutional effect of the 200 μL injection of enoxaparin rather than a treatment-related effect. Alternatively, mice not pretreated with enoxaparin may have been hemoconcentrated slightly due to thrombi and thromboemboli formation, increased vascular permeability, or organ dysfunction in moribund animals. A flaw in the present study was the lack of a control saline only intravenous injection given to untreated mice prior to intracardiac tumor challenge, but it seems unlikely that a 200-μL injection of saline alone would have prevented the rapid thromboemboli formation and subsequent mortality seen in this group.

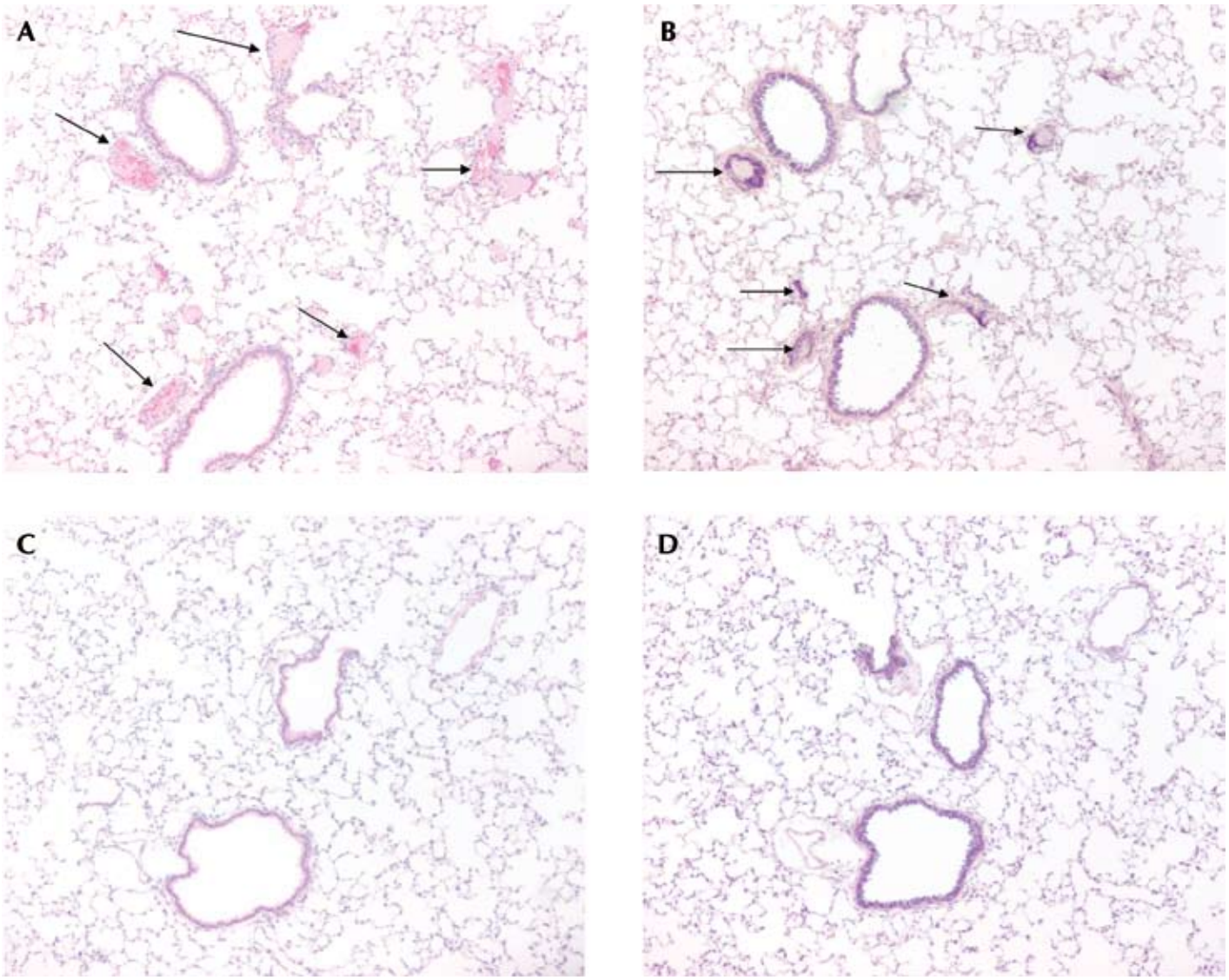


**Figure 3.** Mouse lung. (A, B) No enoxaparin pretreatment. Numerous thrombi (arrows) are seen within the pulmonary vasculature. (C, D) With enoxaparin pretreatment. Thrombi are not present within the pulmonary vasculature. Hematoxylin and eosin stain (A, C); phosphotungstic acid hematoxylin stain (B, D); magnification, ×10.

Taken together, these results demonstrate that intracardiac injection of H2126luc cells induces a hypercoagulable state resulting in a consumption of platelets with extensive pulmonary thromboemboli formation and death. Pretreatment with enoxaparin prevents induction of this hypercoagulable state as demonstrated by normal platelet numbers and a lack of thromboemboli formation.

We evaluated mortality and tumor burden after intracardiac injection of H1975luc and H2126luc to determine whether pretreatment with enoxaparin increased survival or affected tumor burden. In our previous work, injection of $1 \times 10^6$ cells of either of the nonsmall cell lung carcinoma lines H1975luc and H2126luc resulted in consistent and adequate tumor burden, as assessed by bioluminescence, but unacceptably high mortality. When mice were given 10 mg/kg enoxaparin intravenously prior to $1 \times 10^6$ H1975luc tumor challenge, 100% (8 of 8 successfully injected mice) survived, compared with 50% survival (5 of 10 successfully injected mice) of mice without enoxaparin pretreatment. The same enoxaparin dose of 10 mg/kg given subcutaneously prior to intracardiac tumor challenge did not prevent mortality (data not shown). Enoxaparin injection did not produce clinically observable adverse effects and all mice survived to the end of the study (day 29). In addition, pretreatment with enoxaparin had no significant effect on the tumor burden as similar levels of bioluminescence occurred in enoxaparin pretreated and untreated animals. Therefore, 10 mg/kg enoxaparin administered intravenously 10 min prior to intracardiac tumor cell challenge decreased the mortality associated with the H1975luc cells without significantly altering tumor burden.

Our findings with the H1975luc cells were extended to another nonsmall cell lung carcinoma line, H2126luc. An untreated group was not included in this experiment because of the 100% mortality in the H2126luc group that did not receive enoxaparin in the thromboembolism study. Of 12 mice injected, 10 survived the in-

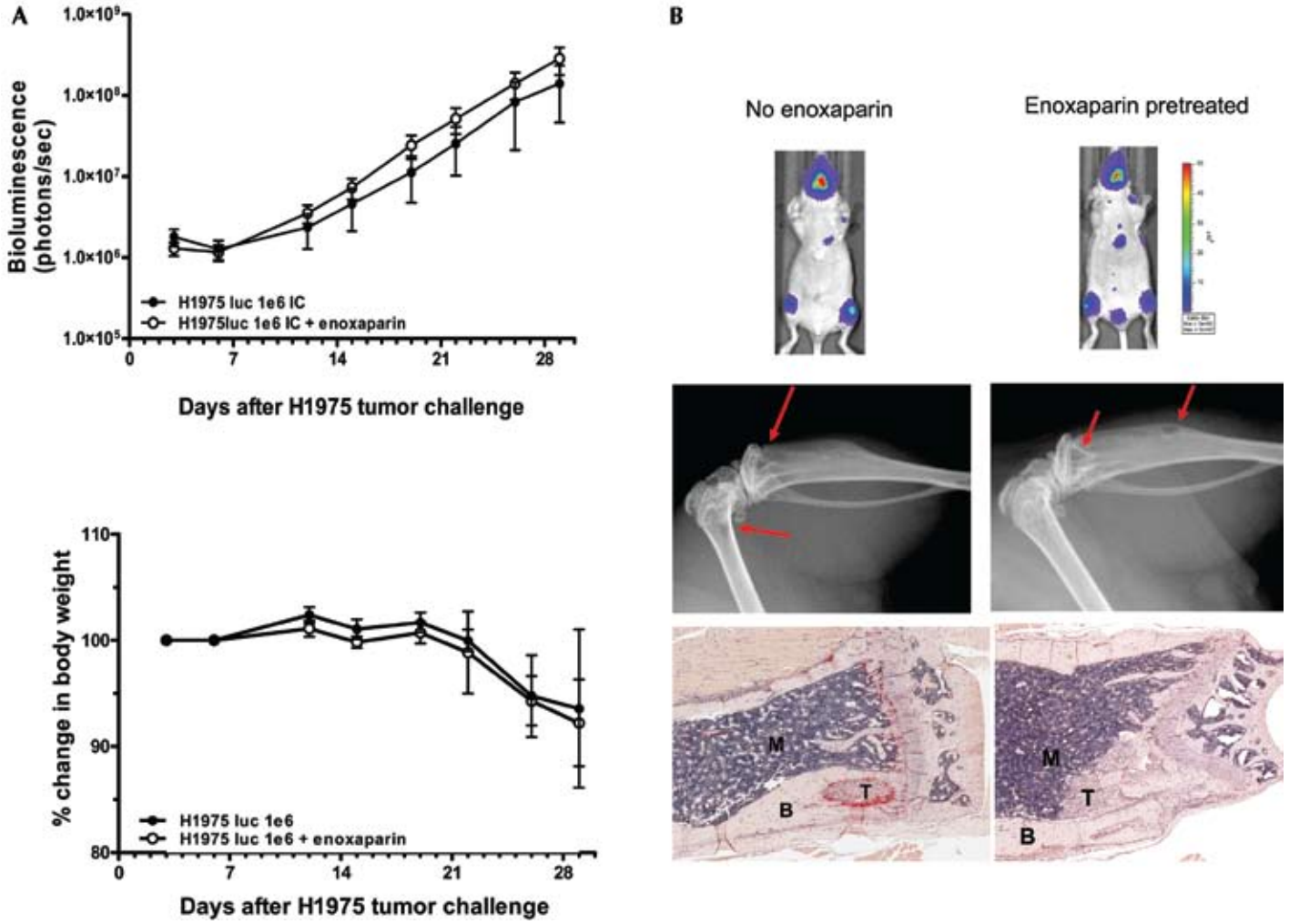


**Figure 4.** H1975 nonsmall cell lung cancer metastases to bone in vivo. (A) Bioluminescent images were captured twice weekly beginning on day 3 after tumor challenge. Data for hindlimb regions are combined values from dorsal and ventral images and plotted as the mean ± SEM for each group (untreated, n = 5; enoxaparin-pretreated, n = 8). Weight loss over the course of the study is plotted as percentage change in body weight relative to day 3 weight. Bioluminescence and weight loss did not differ between groups. (B) No enoxaparin pretreatment (left); enoxaparin pretreatment (right). Top images show mouse photo overlaid with heat map of tumor bioluminescence signal. Color gradation scale ranges from purple (low signal; low tumor burden) to red (high signal; high tumor burden). Units are $10^6$ photons/second/$cm^2$/steradian. The pattern of bioluminescence is similar in animals independent of enoxaparin pretreatment (day 29) and is consistent with tumor growth in the hindlimbs and mandibular bones. Radiographs confirmed the presence of tumor-induced osteolysis (red arrows) that corresponded with BLI signal. Tartrate-resistant acidic phosphatase staining of the hindlimbs revealed the presence osteoclasts at the tumor–bone interface (red). B, bone; M, bone marrow; T, tumor.

tracardiac tumor challenge and were euthanized by day 22 due to 20% body weight loss, severe osteolysis or pathologic fracture. All 10 mice showed acceptable levels of tumor burden and osteolytic lesions in the hindlimbs, as assessed by BLI and radiography. All 9 of the mice euthanized on day 22 had between 1 to 5 foci in each femur and tibia—consistent with what we typically find with successful cell lines in this model. Therefore, pretreatment with enoxaparin before H2126luc intracardiac tumor challenge decreases the mortality previously seen with this cell line while still generating acceptable levels of bone metastases.

Given the results from the current and our previous studies, H2126luc cells may have a greater potential to induce strokes or mortality in the intracardiac model of bone metastasis than do H1975luc cells. The higher (100%) mortality with H2126luc cells could be due to procoagulant factors that are cell-line–specific or to changes to the cells induced by processing prior to injection (for example, trypsinization), but these effects have not been examined.

These experiments showed pretreatment with enoxaparin results in favorable survival rates in mice injected with H1975luc (8 of 8 mice) and H2126luc (10 of 12 mice). The pattern of bioluminescence and development of osteolytic lesions after intracardiac challenge of either H1975 or H2126 was consistent with the development of tumor burden in bone. All enoxaparin-pretreated mice developed the desired metastatic lesions with a pattern of bioluminescent signal in the distal metaphysis of the femur and or proximal metaphysis of the tibia as well as the jaw, similar to the patterns seen in mice that have not received enoxaparin.

The present studies show that intracardiac tumor challenge in nude mice with a human nonsmall cell lung carcinoma cells

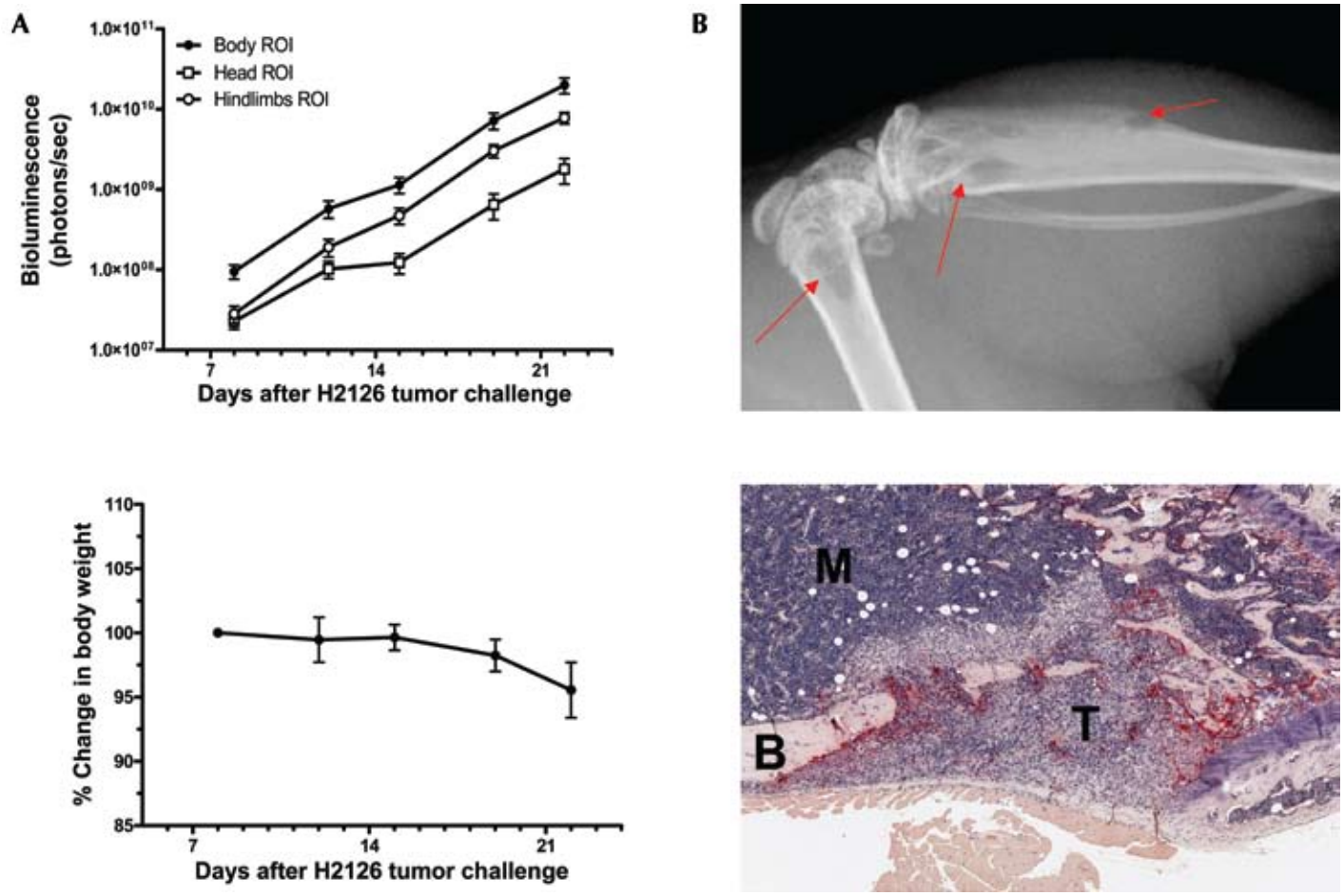


**Figure 5.** H2126 nonsmall cell lung cancer metastases to bone *in vivo.* Monitoring of intracardiac-challenged mice included body weight measurements, BLI, and radiography. (A) The percentage change (mean ± SEM; n = 10) in body weight curve is typical for this model. Body weight is maintained until osteolytic lesions become pronounced. Bioluminescent images were captured twice weekly beginning on day 8 after tumor challenge. Data for whole-body and hindlimb regions are combined values from dorsal and ventral images and plotted as the mean ± SEM for each group (n = 10). Mandibular region data are taken from ventral images. (B) Radiographs confirmed the presence of tumor-induced osteolysis (red arrows) that corresponded with BLI signal. Tartrate-resistant acidic phosphatase staining of the hindlimbs revealed the presence osteoclasts at the tumor–bone interface (red). B, bone; M, bone marrow; T, tumor.

expressing lucerifase and green fluorescence protein can induce a hypercoagulable state leading to a consumption of platelets with thromboemboli formation predominantly in the lungs and that pretreatment with a LMWH will block this state. We postulate that this hypercoagulable state causes the neurologic clinical signs and mortality that occurs after administration of some cell lines. Pretreatment with the LMWH enoxaparin blocks hypercoagulability, prevents adverse clinical signs, and reduces mortality while generating acceptable levels of bone metastases in this model. Therefore, high mortality resulting from intracardiac tumor challenge can be avoided by pretreatment with LMWH without affecting the utility of the metastasis model and thus decreases the number of mice needed for these experiments.

## Acknowledgments

We thank the Pathology Department for their clinical pathology and histology work. We thank Judy Fenyk-Melody and Bill Dougall for their input on this manuscript.

## References

1. **American Cancer Society.** [Internet]. Key statistics about bone metastasis: 2007 update [cited 18 Oct 2007]. Available at http://documents.cancer.org/6119.00/6119.00.pdf.
2. **Andonegui G, Bonder CS, Green F, Mullaly SC, Zbytnuik L, Raharjo E, Kubes P.** 2003. Endothelium-derived Toll-like receptor 4 is the key molecule in LPS-induced neutrophil sequestration into lungs. J Clin Invest **111:**1011–1020.
3. **Andonegui G, Goyert SM, Kubes P**. 2002. Lipopolysaccharide-induced leukocyte-endothelial cell interactions: a role for CD14 versus Toll-like receptor 4 within microvessels. J Immunol **169:**2111–2119.
4. **Andonegui G, Kerfoot SM, McNagny K, Ebbert KVJ, Patel KD, Kubes P.** 2005. Platelets express functional Toll-like receptor 4. Blood **106:**2417–2423.
5. **Arguello F, Baggs RB, Frantz CN**. 1988. A murine model of experimental metastasis to bone and bone marrow. Cancer Research **48**:6876-6881.
6. **Bibby MC**. 2004. Orthotopic models of cancer for preclinical drug evaluation: advantages and disadvantages. European Journal of Cancer **40**:852-857.
7. **Everds NE.** Hematology of the laboratory mouse. In: Fox JG, Barthold SW, Davisson MT, Newcomer CE, Quimby FW, Smith AL, editors.

The mouse in biomedical research, vol. 3. San Diego (CA): Academic Press; 2007. p 133.
8. **Hirsh J, Levine MN.** 1992. Low-molecular–weight heparin. Blood **79:**1–17.
9. **Jenkins DE, Hornig YS, Oei Y, Dusich J, Purchio T.** 2005. Bioluminescent human breast cancer cells lines that permit rapid and sensitive in vivo detection of mammary tumors and multiple metastases in immune deficient mice. Breast Cancer Res **7:**R444–R454.
10. **Jenkins DE, Oei Y, Hornig YS, Yu SF, Dusich J, Purchio T, Contag PR.** 2003. Bioluminescent imaging (BLI) to improve and refine traditional murine models of tumor growth and metastasis. Clin Exp Metastasis **20:**733–744.
11. **Jenkins DE, Yu SF, Hornig YS, Purchio T, Contag PR.** 2003. In vivo monitoring of tumor relapse and metastasis using bioluminescent PC-3M-luc-C6 cells in murine models of human prostate cancer. Clin Exp Metastasis **20:**745–756.
12. **Letai A, Kuter DJ.** 1999. Cancer, coagulation and anticoagulation. Oncologist **4:**443–449.
13. **Lip GYH, Chin BSP, Blann AD.** 2002. Cancer and the prothrombotic state. Lancet Oncol **3:**27–34.
14. **Miller FR, Medina D, Heppner GH**. 1981. Preferential growth of mammary tumors in intact mammary fatpads. Cancer Research **41**:3863-3867.
15. **Miller R.** 2007. Personal communication.
16. **Momi S, Nasimi M, Colucci M, Nenci GG, Gresele P.** 2001. Low molecular weight heparins prevent thrombin-induced thromboembolism in mice despite low anti-thrombin activity. Evidence that the inhibition of feedback activation of thrombin generation confers safety advantages over direct thrombin inhibition. Haematologica **86:**297–302.
17. **Moore DM.** Hematology of the mouse. In: Feldman BF, Zinkl, JG, and Jain NC, editors. Schalm's veterinary hematology. Balto (MD): Lippincott, Williams, and Wilkins; 2000. p 1219.
18. **Morony S, Capparelli C, Sarosi I, Lacey D, Dunstan CR, Kostenuik PJ.** 2001. Osteoprotegerin inhibits osteolysis and decreases skeletal tumor burden in syngeneic and nude mouse models of experimental bone metastasis. Cancer Res **61:**4432–4436.
19. **Mousa SA, Linhardt R, Francis JL, Amirkhosravi A.** 2006. Antimetastatic effect of a non-anticoagulant low-molecular-weight heparin versus the standard low-molecular-weight heparin, enoxaparin. Thromb Haemost **96:**816–821.
20. **Mundy GR.** 2002. Metastasis to bone: causes, consequences and therapeutic opportunities. Nat Rev Cancer **2:**584–593.
21. **National Research Council**. Guide for the care and use of laboratory animals. Washington (DC): National Academic Press; 1996.
22. **Paul W, Gresele P, Momi S, Bianchi G, Page CP.** 1993. The effect of defibrotide on thromboembolism in the pulmonary vasculature of mice and rabbits and in the cerebral vasculature of rabbits. British Journal of Pharmacology **110**:1565-1571.
23. **Rosol TJ, Tannehill-Gregg SH, LeRoy BE, Mandl S, Contag CH.** 2003. Animal models of bone metastasis. Cancer **97 Suppl:**748–757.
24. **Rubens RD.** 1998. Bone metastases-the clinical problem. Eur J Cancer **34:**210–213.
25. **Sehgal I, Foster TP, Francis J**. 2006. Prostate cancer cells show elevated urokinase receptor in mouse model of metastasis. Cancer Cell International **6**:21-29.
26. **Slofstra SH, Bijlsma MF, Groot AP, Reitsma PH, Lindhout T, ten Cate H, Spek CA.** 2007. Protease-activated receptor-4 inhibition protects from multiorgan failure in a murine model of systemic inflammation. Blood **110:**3176–3182.
27. **Slofstra SH, van't Veer C, Buurman WA, Reitsma PH, ten Cate H, Spek CA.** 2005. Low molecular weight heparin attenuates multiple organ failure in a murine model of disseminated intravascular coagulation. Crit Care Med **33:**1365–1370.
28. **Smorenburg SM, Van Noorden CJF.** 2001. The complex effects of heparins on cancer progression and metastasis in experimental studies. Pharmacol Rev **53:**93–105.
29. **Tsakiris DA, Scudder L, Hodivala-Dilke K, Hynes RO, Coller BS.** 1999. Hemostasis in the mouse (*Mus musculus*): a review. Thromb Haemost **81:**177–188.
30. **Vicent S, Luis-Ravelo D, Antón I, García-Tuñón I, Borrás-Cuesta F, Dotor J, De Las Riva J, Lecanda F.** 2008. A novel lung cancer signature mediates metastatic bone colonization by a dual mechanism. Cancer Res **68:**2275–2285.
31. **Whitehurst B, Flister MJ, Bagaitkar J, Volk L, Bivens CM, Pickett B, Castro-Rivera E, Brekken RA, Gerard RD, Ran S**. 2007. Anti-VEGF-A therapy reduces lymphatic vessel density and expression of VEGFR-3 in an orthotopic breast tumor model. International Journal of Cancer **121**:2181-2191.